Biointerface Research in Applied Chemistry
Open-Access Journal (ISSN: 2069-5837)

Article
Volume 16, Issue 3, 2026, 75
https://doi.org/10.33263/BRIAC163.075

Molecular Docking and Network Pharmacology Interaction Analysis of Water Lily Seed Extract (*Nymphaea pubescens* Willd) with Target Inhibitory Mechanism in Alzheimer's Disease

Dinda Fadhilah Belahusna [1], Putra Santoso [1,*], Resti Rahayu [1]

[1] Biology Department Faculty of Mathematics and Natural Sciences, Universitas Andalas, Padang 25163 Indonesia
* Correspondence: putrasantoso@sci.unand.ac.id;

Received: 19.02.2026; Accepted: 18.05.2026; Published: 15.06.2026

Abstract: Alzheimer's disease (AD) is a progressive neurodegenerative disorder characterized by cognitive decline and limited therapeutic options. Targeting amyloid precursor protein (APP) processing and butyrylcholinesterase (BChE) activity is considered a promising strategy for AD treatment. This study investigated the potential molecular mechanisms of the water lily seed (Nymphaea pubescens Willd.) ethanolic extract in AD using network pharmacology and molecular docking. Bioactive compounds and their targets were identified from the SEA, DisGeNET, and Open Targets databases, followed by construction of a protein–protein interaction network, gene ontology, and KEGG pathway enrichment analyses. Molecular docking was performed to assess interactions between selected compounds and key AD-related targets. Five overlapping genes were identified, with APP and BChE showing high centrality in the network. Docking results indicated predicted binding interactions of major compounds to APP and BChE, with binding energies ranging from −6.0 to −7.9 kcal/mol. These binding energy values should be interpreted cautiously as preliminary computational predictions. *In silico* pharmacokinetic analysis indicated acceptable drug-likeness properties. Overall, the findings indicate that compounds from *N. pubescens* seed extract may interact with multiple AD-related targets at the computational level; however, these results remain preliminary and require further experimental validation.

Keywords: *Nymphaea pubescens*; network pharmacology; molecular docking; APP; BChE.

1. Introduction

Alzheimer's disease (AD) is a progressive, age-related neurodegenerative disorder and the leading cause of dementia worldwide. Its prevalence increases sharply with advancing age, making population aging a major contributor to the growing global burden of the disease [1]. Clinically, AD is characterized by gradual cognitive decline and memory impairment, while pathologically it involves synaptic dysfunction and neuronal loss in brain regions critical for learning and memory, including the hippocampus, entorhinal cortex, and cerebral cortex [2].

One of the central pathological hallmarks of AD is the accumulation of extracellular amyloid-β (Aβ) plaques, which are generated by sequential cleavage of the amyloid precursor protein (APP) by β- and γ-secretases [3]. APP exists in several isoforms, with APP695

predominantly expressed in neurons, while APP751 and APP770 are mainly localized in glial cells [4,5]. Under physiological conditions, APP plays an essential role in neuronal growth and synaptic maintenance [2]. However, aberrant APP processing leads to excessive amyloid-β (Aβ) production, which aggregates and induces oxidative stress, neuroinflammation, and neuronal degeneration, ultimately impairing neurotransmission and cognitive function [3]. The extracellular E2 domain of APP contributes to APP dimerization and structural stabilization, processes that can influence APP conformation and its susceptibility to proteolytic processing [6]. Structural studies have shown that the E2 domain forms a conserved antiparallel dimer interface involved in ligand-mediated interactions. Therefore, investigating molecular interactions within this domain may provide insight into compounds that interact with structural regions of APP associated with Alzheimer's disease pathology [7].

In addition, cholinergic dysfunction represents a major neurochemical alteration in AD. Butyrylcholinesterase (BChE), whose activity increases in advanced stages of the disease, has been shown to accelerate Aβ aggregation and exacerbate cognitive deficits, highlighting its importance as a therapeutic target [8]. BChE also contributes to acetylcholine hydrolysis when acetylcholinesterase activity declines during disease progression, making it an important target for improving cholinergic neurotransmission in AD [9]. Despite extensive research, currently available pharmacological treatments for AD remain largely symptomatic and do not effectively halt disease progression. This limitation has stimulated increasing interest in natural products and medicinal plants as potential sources of multi-target agents capable of modulating the complex pathological pathways involved in AD.

Nymphaea pubescens Willd (water lily) is a medicinal plant widely used in traditional medicine for the treatment of various ailments, including diabetes, inflammation, diarrhea, and dysentery [10]. Phytochemical studies have demonstrated that *N. pubescens* is rich in bioactive compounds, including alkaloids, flavonoids, phenolics, terpenoids, tannins, and saponins [11]. Previous reports showed that water lily leaves possess antidiabetic and hypolipidemic properties [12], while the flowers exhibit antioxidant and anti-inflammatory activities in experimental models [13]. Furthermore, related species within the Nymphaeaceae family, including *Nymphaea lotus*, have been reported to enhance learning and memory in animal models, suggesting potential neuroprotective effects [14].

Previous computational studies on *Nymphaea* species have primarily focused on metabolic and inflammatory disorders rather than neurodegenerative diseases. For instance, Oyeyemi *et al.* reported that several phytochemicals from *Nymphaea lotus* showed promising binding affinities toward diabetes-related targets through molecular docking and molecular dynamics simulations, suggesting potential antidiabetic and anti-inflammatory mechanisms [15]. Similarly, Ishrat *et al.* demonstrated the antidiabetic activity of *Nymphaea rubra* flower constituents through combined in vitro, in vivo, and in silico analyses targeting metabolic enzymes [16]. While these studies highlight the pharmacological potential of *Nymphaea*-derived phytochemicals, they primarily examine metabolic pathways and do not assess their interactions with neurodegenerative disease targets, such as the amyloid precursor protein (APP) or cholinesterase enzymes.

Recent advances in computational biology have enabled in silico approaches, such as molecular docking, to explore interactions between bioactive compounds and disease-related targets at the molecular level. Molecular docking provides valuable insights into ligand–protein binding affinity and interaction modes, facilitating early-stage identification of promising

therapeutic candidates [15]. Given the multifactorial nature of AD, this approach is particularly useful for investigating multi-target mechanisms of plant-derived compounds.

However, to date, there is limited evidence regarding the neuroprotective potential of *N. pubescens* seeds against AD-related molecular targets. Therefore, this study aimed to investigate the potential interactions between compounds identified in *N. pubescens* seed extract and AD-related targets, particularly APP and BChE, using network pharmacology and molecular docking approaches. We hypothesized that selected bioactive compounds from *N. pubescens* seeds may exhibit predicted binding interactions with these targets, providing preliminary insights into their potential multi-target relevance in AD-related pathways.

2. Materials and Methods

2.1. Phytochemical identification of Nymphaea pubescens seeds.

The phytochemical constituents analyzed in this study were obtained from LC-MS and GC-MS profiling of *Nymphaea pubescens* seed extract conducted by the authors. The experimental analyses were performed as part of an ongoing phytochemical investigation. The detailed analytical procedures and full compound characterization are currently under peer review in a separate manuscript. Only compounds experimentally detected in the LC-MS and GC-MS datasets with identifiable molecular formulas and PubChem records were included in the subsequent ADME, network pharmacology, and molecular docking analyses. This approach ensured that the analyzed phytochemical dataset was based exclusively on experimentally detected compounds rather than predicted phytochemicals from literature sources.

2.2. ADME and toxicity prediction.

The pharmacokinetic properties of the identified compounds were evaluated using *in silico* ADME analysis. Two-dimensional structures and SMILES codes were retrieved from PubChem and analyzed using SwissADME (http://www.swissadme.ch) to predict gastrointestinal absorption and Lipinski's rule of five. Blood–brain barrier permeability, volume of distribution (VDss), and central nervous system permeability were predicted using pkCSM (http://biosig.lab.uq.edu.au/pkcsm). Compounds were interpreted using commonly applied pkCSM thresholds, where logBB > 0.3 indicates high BBB permeability and logBB < −1.0 indicates poor penetration, while CNS permeability values (logPS) greater than −2 suggest potential CNS accessibility. VDss predictions were interpreted based on pkCSM classification, where logVDss > 0.45 indicates high distribution and logVDss < −0.15 indicates low distribution. In addition, toxicity profiles of the compounds were assessed using ProTox-II (http://tox-new.charite.de/protox_II).

2.3. In silico analysis of bioactive compounds.

Biological activity was predicted using the Prediction of Activity Spectra for Substances (PASS) Online server (http://www.way2drug.com/passonline). The Simplified Molecular Input Line Entry System (SMILES) of each compound was obtained from the PubChem database and submitted to PASS Online for activity prediction. Predicted activities were interpreted based on the probability of activity (Pa) values, where Pa > 0.7 indicated a high likelihood of experimental activity, 0.5 < Pa < 0.7 suggested moderate probability, and Pa

< 0.5 indicated low probability of biological activity. However, PASS predictions are statistical estimates based on structure-activity relationships and may yield false positives; therefore, the results were interpreted cautiously and used primarily as preliminary screening criteria rather than definitive indicators of biological activity.

2.4. Prediction of protein targets and gene-disease associations

Target proteins were analyzed using the SEA Search Server (https://sea.bkslab.org/) [17]. While the list of proteins/genes associated with Alzheimer's disease was obtained from the DisGeNET database (https://www.disgenet.org/search) [18] and Open Target (https://www.opentargets.org/). Protein targets obtained from SEA were intersected with AD-related genes retrieved from DisGeNET and Open Targets to identify overlapping targets. Only proteins appearing in at least two databases or showing strong disease association scores were retained. This filtering process identified 32 proteins deemed relevant for subsequent network and docking analyses.

2.5. Graph topological networks.

The compilation of target protein lists from both databases is then input into the multiple protein menu from the STRING database (https://string-db.org/). In addition, additional settings in the form of selecting the type of organism are set to Homo sapiens, the meaning of network edges is used as confidence, and the minimum required interaction score is set to 0.700 (high confidence). After the network is updated with these additional settings, the visualization results are downloaded in TSV (tab-separated values) format from the table/export menu. The downloaded file (.tsv) is then imported into the Cytoscape v.3.9.0 software to then proceed to the analyze network procedure on the tools menu. The Network Analyst server (https://www.networkanalyst.ca/NetworkAnalyst/) [19] was also used to construct an association network with Alzheimer's.

2.6. Analysis of modes of actions.

The mechanism of action of the bioactive compounds from each herb was analyzed using the Comparative Toxicogenomic Database/CTD (http://ctdbase.org/voc.go?type=chem) [20]. Proteins with fewer than three interactions were eliminated to obtain highly valid data. Target protein analysis was also performed using the STITCH database (http://stitch.embl.de/). STITCH analysis is performed by entering the name of the compound in the multiple names menu at STITCH. Then, additional settings were made by selecting the type of organism to be Homo sapiens, and the required minimum interaction score was changed to 0.700. Annotation of gene and protein lists was performed using DAVID (Database for Annotation, Visualization, and Integrated Discovery) (https://david.ncifcrf.gov/home.jsp) [21]. A significant value of $p < 0.05$ is used to select the biological processes and pathways most potentially related to Alzheimer's treatment.

2.7. Ligand preparation.

Ligands selected based on PASS Online and SwissADME screening were prepared using BIOVIA Discovery Studio. The ligand structures were downloaded from the PubChem database in SDF format and imported into the software for standardization and saving prior to further analysis.

2.8. Protein preparation.

The three-dimensional structures of the target proteins, butyrylcholinesterase (BChE; PDB ID: 4BDS) and amyloid precursor protein (APP; PDB ID: 3UMI), were retrieved from the Protein Data Bank (PDB). The three-dimensional structures of the active compounds and control ligands were obtained from the PubChem database for subsequent molecular interaction studies.

2.9. Docking analysis.

The 3D structures of the target proteins are BChE (PDB ID: 4BDS) and APP (PDB ID: 3UMI) proteins taken from the PDB database, while the 3D structures of the active and control compounds were obtained from the PubChem database (https://www.pubchem.ncbi.nlm.nih.gov). Furthermore, the protein was prepared by removing water molecules and ligands in the Discovery Studio 2019 software, while the energy minimization of the ligands was carried out using PyRx v.0.9.8 software.

Docking was performed using AutoDock Vina integrated in PyRx v.0.9.8. The targeted docking approach was applied with an exhaustiveness parameter of 50 to enhance sampling of ligand conformations within the binding site. AutoDock Vina generated nine binding poses for each ligand–protein complex, and the pose with the lowest predicted binding affinity was selected for subsequent interaction analysis. The grid box parameters were defined to encompass the predicted binding pocket of each target protein fully. For BChE (PDB ID: 4BDS), the grid box was centered on the catalytic gorge based on the position of the co-crystallized ligand reported in the crystal structure. For APP (PDB ID: 3UMI), the grid box was positioned according to the most probable ligand-binding pocket predicted using the PrankWeb server. The center coordinates and dimensions of the docking grid boxes are presented in Table 1.

Table 1. Center and dimension gridbox docking.

Protein	Center			Dimension		
	x	y	z	x	y	z
BChE (4BDS)	135,4764	116,1602	40,3167	7,5	10	10
APP (3UMI)	-56,8633	-35,7824	-15,2185	20	20	20

The docking results are presented as binding affinities and interactions between the compounds and the docked proteins, which are visualized in BioVia Discovery Studio 2019. It should be noted that the AutoDock Vina scoring function provides approximate binding affinity predictions based on empirical scoring algorithms and may not fully capture all thermodynamic contributions to ligand binding. Therefore, docking results were interpreted as relative binding estimates rather than absolute binding energies.

2.10. Docking validation.

Redocking validation was performed for BChE (PDB ID: 4BDS) by re-docking the co-crystallized ligand into the active site using the same docking parameters. The grid box was optimized to cover the native binding pocket, and the redocking procedure confirmed that the docking protocol was able to reproduce the binding pose of the native ligand within the acceptable RMSD threshold (< 2 Å), indicating the reliability of the docking method used in this study.

For APP (PDB ID: 3UMI), conventional redocking could not be performed because the crystal structure does not contain a co-crystallized small-molecule ligand. Therefore, binding site prediction was performed using the PrankWeb server to identify the most probable ligand-binding pocket prior to docking analysis. Post-docking filtering was performed by selecting ligand poses with the lowest binding affinity values and analyzing key intermolecular interactions, including hydrogen bonds, hydrophobic interactions, and aromatic interactions.

3. Results and Discussion

3.1. ADME prediction related to neuroprotective potential.

Based on the experimentally detected compounds obtained from LC-MS and GC-MS profiling of *Nymphaea pubescens* seed extract, ADME prediction (Table 2) was performed to evaluate pharmacokinetic parameters, including GI absorption, Lipinski's rule of five, VDss, BBB permeability, CNS permeability, and toxicity. Several compounds, particularly chalcone, ellagic acid glucoside, 2,4,6-trihydroxybenzoic acid, and 8-demethyleucalyptin, showed relatively favorable pharmacokinetic properties and satisfied the predefined drug-likeness criteria. Among these, chalcone fulfilled Lipinski's rule of five [22] and exhibited predicted BBB permeability (logBB > 0.3), suggesting potential suitability for central nervous system exposure [23] 8-Demethyleucalyptin and 2,4,6-trihydroxybenzoic acid also exhibit favorable pharmacokinetic profiles, while ellagic acid glucoside showed poor predicted BBB permeability (logBB < −1) which is consistent with the limited brain penetration generally associated with highly polar glycosylated compounds [24]. Although docking analysis indicated a strong binding affinity of ellagic acid glucoside toward the target protein, its limited predicted BBB permeability may restrict direct central nervous system activity. Therefore, compound prioritization in this study was based on an integrated assessment of both docking affinity and ADME properties. Overall, these ADME predictions represent preliminary computational estimations and should be interpreted cautiously, as experimental pharmacokinetic validation is required to confirm compound bioavailability and brain penetration.

Table 2. Pharmacokinetic and toxicity prediction of compounds identified using SwissADME, pkCSM, and ProTox-II.

Compound name	SwissADME		pkCSM		ProTox-II	
	Lipinski	VDss (human) (log L/kg)	BBB permeability (log BB)	CNS permeability (log PS)	Predicted LD_{50} (mg/kg)	Predicted toxicity class
Propionic acid	**Yes; 0 violations**	**-0.756**	**-0.292**	**-2.615**	**300**	**3**
Chalcone	**Yes; 0 violations**	**0.365**	**0.56**	**-1.243**	**1048**	**4**
Cyclotrisiloxane, hexamethyl-	**Yes; 0 violations**	**-0.131**	**0.205**	**-2.987**	**24134**	**6**
Butanoic acid	**Yes; 0 violations**	**-0.831**	**-0.258**	**-2.537**	**91**	**3**
Ergosta-5,22-dien-3-ol, acetate, (3.beta.,22E)-	Yes; 0 violations	0.278	0.724	-1.745	1185	4
91485-02-8 3,4,8,9,10-Pentahydroxybenzo[c]chromen-6-one	Yes; 0 violations	1.534	-1.318	-3.114	2991	4
Ellagic acid glucoside	**Yes; 0 violations**	**0.616**	**-1.881**	**-4.572**	**5000**	**5**
Phyllanthusiin E	Yes; 0 violations	-0.587	-1.246	-3.436	5000	5
Butylidenephthalide	Yes; 0 violations	0.336	0.182	-1.799	1850	4
2,4,6-trihydroxybenzoic acid	**Yes; 0 violations**	**-0.742**	**-1.082**	**-3.346**	**1250**	**4**
Emblicanin A	Yes; 0 violations	0.139	-3.709	-5.526	10000	6
Limonin	Yes; 0 violations	0.265	-0.844	-3.07	244	3

Compound name	SwissADME		pkCSM		ProTox-II	
	Lipinski	VDss (human) (log L/kg)	BBB permeability (log BB)	CNS permeability (log PS)	Predicted LD_{50} (mg/kg)	Predicted toxicity class
Physalin O	Yes; 1 violations: MW>500	0.584	-0.78	-3.081	800	4
D-Pinitol	**Yes; 0 violations**	**-0.213**	**-1.053**	**-4.019**	**804**	**4**
Matairesinol	Yes; 0 violations	-0.265	-0.49	-3.071	1500	4
Leonoside E	No; 3 violations: MW>500, NorO>10, NHorOH>5	0.234	-1.74	-5.232	5000	5
8-Demethyleucalyptin	**Yes; 0 violations**	**0.045**	**-0.297**	**-2.059**	**3919**	**5**
Biphenylindanone A	Yes; 1 violations: MLOGP>4.15	-2.164	-0.128	-1.527	10000	6
3-tert-Butyl-4-hydroxyanisole	Yes; 0 violations	0.229	0.361	-1.559	880	4
Broussoflavan A	Yes; 0 violations	0.66	-0.95	-2.785	2500	5
Physagulin A	Yes; 1 violations: MW>500	0.075	-0.625	-2.965	400	4
Hydrocortisone hemisuccinate	Yes; 0 violations	-0.565	-1.023	-3.287	3000	5
25(R)-Hydroxyprotopa-naxadiol	Yes; 1 violations: MLOGP>4.15	-0.363	-0.639	-2.017	1190	4
Trilobolide	Yes; 1 violations: MW>500	-0.384	-0.739	-3.479	7	2
3-O-vanillyceanothic acid	No; 2 violations: MW>500, MLOGP>4.15	-1.52	-0.998	-2.879	3700	5
Linolenic Acid	Yes; 1 violations: MLOGP>4.15	-0.617	-0.115	-1.547	10000m	6
Galactaric acid	**Yes; 1 violation: NHorOH>5**	**-0.477**	**-1.259**	**-4.224**	**9100**	**6**
2,2'-Ethylidenebis(4,6-di-tert-butylphenol)	Yes; 1 violations: MLOGP>4.15	-0.284	-0.845	-1.115	10000	6
Palmitoleoyl and linoleoyl	No; 2 violations: MW>500, MLOGP>4.15	-0.913	-0.894	-2.938	11210	6
1-palmitoyl-2-arachidonoyl-sn-glycerol	No; 2 violations: MW>500, MLOGP>4.15	-1.014	-0.901	-2.902	11210	6
Nuatigenin 3-beta-D-glucopyranoside	Yes; 1 violations: MW>500	-0.412	-1.011	-1.011	8000	6
22-Acetylpriverogenin B	No; 2 violations: MW>500, MLOGP>4.15	0.247	-0.08	-1.379	5000	5
Acetoxolone	No; 2 violations: MW>500, MLOGP>4.15	-1.375	-0.134	-1.219	3300	5
Tetra-hydroxyethyl-quercetin	No; 2 violations: NorO>10, NHorOH>5	0.776	-2.716	-4.315	5000	5
Euparotin acetate	Yes; 0 violations	-0.111	-0.798	-3.071	400	4

Compounds shown in **bold** meet the docking criteria based on SwissADME and pkCSM analyses. VDss values are considered low if < −0.15 and high if > 0.45. Compounds with logBB > 0.3 are considered capable of readily crossing the blood–brain barrier (BBB), whereas those with logBB < −1 are poorly distributed to the brain. Compounds with CNS permeability values of logPS > −2 are considered able to penetrate the central nervous system (CNS), while those with logPS < −3 are considered unable to penetrate the CNS.

3.2. PASS online bioactivity prediction.

Based on the PASS Online analysis (Figure 1), the predicted bioactivities of compounds identified in *the N. pubescens seed extract suggest* potential multi-target neuroprotective mechanisms. Several compounds exhibited strong predicted activity (Pa > 0.7) against key targets. Notably, ellagic acid glucoside demonstrated high probable activity as a lipid peroxide

inhibitor (Pa = 0.80), antioxidant (Pa = 0.75), and anti-inflammatory agent (Pa = 0.73), aligning with established pathways for mitigating oxidative stress and neuroinflammation in neurodegenerative diseases [25]. Furthermore, its predicted inhibition of JAK2 expression (Pa = 0.70) suggests a potential role in modulating the neuroinflammatory JAK-STAT signaling pathway associated with neuroinflammatory responses [26].

Other compounds showed specific, high-probability activities. Galactaric acid was predicted as a potent antioxidant (Pa = 0.75). Chalcone, the lead candidate from ADME analysis, was predicted to be a strong GABA aminotransferase inhibitor (Pa = 0.71), indicating a potential mechanism to enhance GABAergic neurotransmission, which is often dysfunctional in epilepsy and anxiety disorders [27]. However, PASS predictions represent probabilistic estimations of biological activity and are associated with potential false-positive rates. Therefore, these predictions should be interpreted cautiously and require experimental validation.

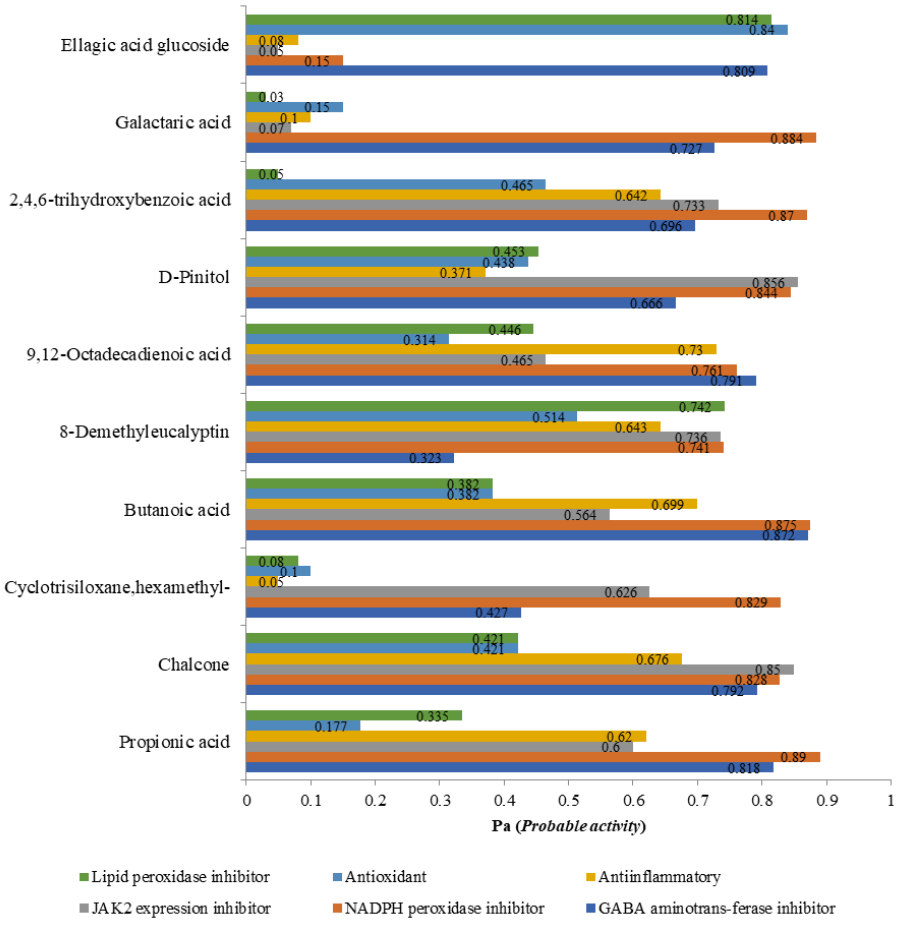

Figure 1. Predicted bioactivity of compounds from *N. pubescens* seed extract based on PASS Online analysis.
Note: A Pa value > 0.7 indicates a high probability of biological activity under experimental conditions and suggests that the tested compounds may act as analogs of existing drugs.

3.3. Prediction of protein targets and gene-disease associations.

For visualization purposes, each compound was coded by its first two letters (Table 3). In the visual representation, green indicates predicted target proteins identified exclusively in the Comparative Toxicogenomics Database (CTD), whereas orange indicates targets predicted exclusively by SEA Target.

Gene-disease association analysis revealed that nine target proteins in lotus seeds were associated with Alzheimer's disease in the Open Targets (OT) database. Additionally, eighteen

target proteins were identified as associated with Alzheimer's disease based on the DisGeNET (DG) database. Significantly, a core subset of five target proteins was commonly identified by both independent databases (Figure 2), reinforcing their high-confidence relevance to Alzheimer's disease pathology [28].

A total of 32 target proteins, derived from the combination of OT and DG results, were selected for subsequent graph topological network analysis. Further analysis demonstrated that several key targets could be modulated by more than one bioactive compound from N. pubescens seeds (Table 4), suggesting a synergistic, polypharmacological mechanism of action characteristic of natural products [29].

Table 3. Ligand compound codes from *N. pubescens* seed extract.

Compound	CODE	CID
Propionic acid	PR	1032
Chalcone	CH	637760
Cyclotrisiloxane, hexamethyl-	CY	10914
Butanoic acid	BU	264
8-Demethyleucalyptin	DE	15715157
9,12-Octadecadienoic acid	OC	3931
D-Pinitol	PI	164619
2,4,6-trihydroxybenzoic acid	TR	66520
Galactaric acid	GA	3037582
Ellagic acid glucoside	EL	91072206

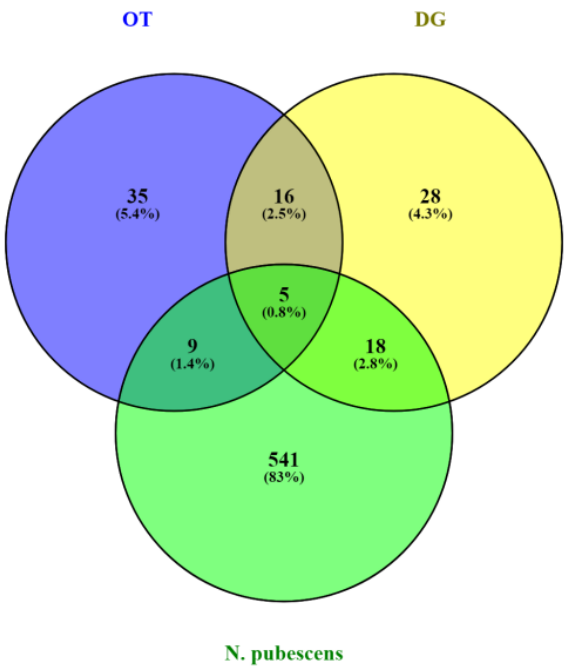

Figure 2. Cross-targets between target proteins from 9 herbal samples and a list of proteins associated with NP (*N. pubescens*), OT (Open Target), and DG (DisGeNET).

Table 4. Tabulation of target proteins of bioactive compounds of *N. pubescens* samples associated with Alzheimer's.

NP-OT-DG	
APP	DE
ACHE	CH-DE
BCHE	CH-OC
BIN1	BU
PPARG	CH-BU-OC
NP-OT	
GRIN2A	OC
GRIN2B	OC
PTGS2	CH-BU-DE-OC
PTGS1	CH-BU

HMGCR	BU-OC
SLC6A3	BU
GABBR1	BU
GABBR2	BU
SCN9A	BU
NP-DG	
IL1B	PR-CH-BU-OC-PI
INSR	OC
LEP	BU
BCL2	PR-CH-BU-OC
CASP3	PR-CH-BU-OC
BAX	CH-BU
NOS3	OC
CHRNA7	OC
CYP2D6	BU
ESR1	DE
HMOX1	CH-OC
IGF1	BU
IL6	PR-CH-BU-OC-PI
MAOB	CH-DE
PRNP	BU
TFAM	PR
TNF	PR-CH-BU-OC-PI
VEGFA	PR-BU-OC

NP (*N. pubescens*); OT (Open Targets), DG (DisGeNET). Proteins highlighted in purple indicate targets identified in the topological network graph.

3.4. Graph topological networks.

Topological graph analysis was performed using two databases, STRING and NetworkAnalyst. Results from NetworkAnalyst revealed that of the 32 input proteins, only 12 were identified as directly related to Alzheimer's disease (Figure 3).

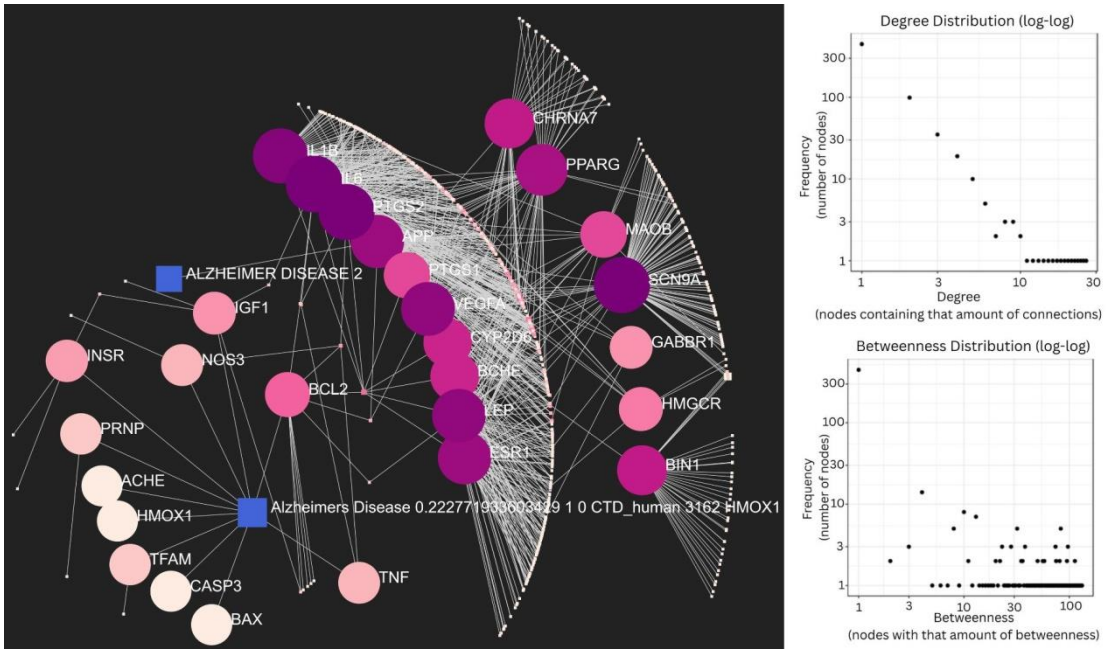

Figure 3. Results of graph topological network analysis with NetworkAnalyst of herbal target proteins associated with Alzheimer's. Notes that have a position closer to the center, a large node size, and have an edge/line directly with Alzheimer's (blue box), the dominance and role of this protein is higher and more important.

Visualization in NetworkAnalyst was conducted using a concentric-circle layout, where nodes closer to the center indicate higher centrality and stronger association with Alzheimer's

disease. According to the NetworkAnalyst analysis, the twelve target proteins with the highest centrality and strongest associations were APP, ACHE, BCHE, INSR, BCL2, CASP3, BAX, NOS3, HMOX1, IGF1, PRNP, and TFAM. These proteins are well-documented core players in Alzheimer's disease pathogenesis, involving amyloid-beta metabolism, cholinergic deficit, apoptosis, oxidative stress, and insulin signaling pathways [30].

Prediction of protein targets and gene-disease associations was performed for ten bioactive compounds from *N. pubescens* seeds, with each compound coded using the first two letters of its name for visualization purposes. Data mining revealed that nine target proteins were associated with Alzheimer's disease according to the Open Targets database, while eighteen proteins were associated according to DisGeNET, with five proteins overlapping between the two databases, resulting in a total of 32 proteins selected for further analysis. Graph topological networks were constructed using STRING and NetworkAnalyst, with NetworkAnalyst's visualization employing a concentric-circle layout, indicating that nodes closer to the center have higher centrality and stronger associations with Alzheimer's disease. Among the 32 proteins, twelve (APP, ACHE, BCHE, INSR, BCL2, CASP3, BAX, NOS3, HMOX1, IGF1, PRNP, and TFAM) demonstrated the highest centrality and were prioritized for detailed network analysis.

Network analysis further assessed protein-protein interactions using key parameters, including Degree, Betweenness Centrality, and Closeness Centrality, to identify hub proteins that may serve as regulatory centers within Alzheimer 's-related biological processes. Degree centrality reflected the number of interactions per protein, betweenness centrality identified nodes on the shortest paths, and closeness centrality measured accessibility within the network. Based on these metrics, the most influential target proteins were ranked (Table 5), and 24 of the 32 proteins were found to form a common interaction cluster (Figure 4), highlighting their potential as multi-target candidates for Alzheimer's therapy. The identification of CASP3 and APP as nodes with relatively high betweenness centrality suggests that these proteins may occupy important positions within the interaction network. However, centrality values alone do not establish biological dominance and should be interpreted within the broader context of network topology [31].

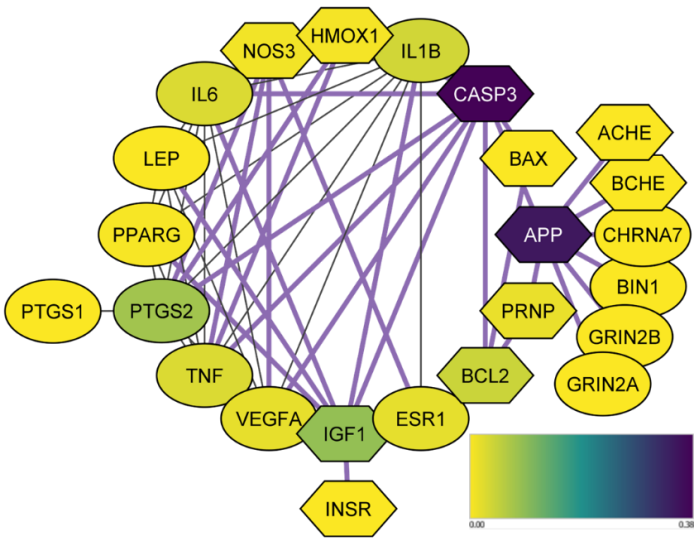

Figure 4. Results of graph topological network analysis with STRING of herbal target proteins associated with Alzheimer's. The closer to the purple color, the higher and more important the dominance and role of the protein. Nodes with hexagon shapes mark target proteins associated with Alzheimer's based on analysis from NetworkAnalyst.

Table 5. Results of tabulated graph topological network analysis between STRING and NetworkAnalyst, which shows the most dominant protein sequences that play a role in the pathways of the Alzheimer's treatment mechanism.

Protein	Betweenness centrality	Closeness centrality	Degree	Stress
CASP3	0.51981	0.638889	10	582
APP	0.479578	0.522727	8	464
IGF1	0.122219	0.511111	9	166
PTGS2	0.106559	0.511111	9	128
BCL2	0.057971	0.442308	4	94
IL1B	0.050348	0.534884	10	112
TNF	0.038745	0.534884	10	100
IL6	0.038745	0.534884	10	100
ESR1	0.024657	0.410714	4	40
VEGFA	0.02349	0.511111	8	62
PRNP	0.020751	0.383333	2	28
NOS3	0.01054	0.410714	6	14
HMOX1	0.007642	0.479167	6	20
PPARG	0.004216	0.403509	6	12
LEP	6.59E-04	0.396552	6	2
PTGS1	0	0.343284	1	0
INSR	0	0.343284	1	0
BAX	0	0.418182	2	0
BIN1	0	0.348485	1	0
GRIN2B	0	0.353846	2	0
CHRNA7	0	0.348485	1	0
GRIN2A	0	0.353846	2	0
BCHE	0	0.348485	1	0
ACHE	0	0.348485	1	0

3.5. Analysis of modes of action.

Network pharmacology analysis and gene-disease associations revealed that the target proteins APP, AChE, and BChE were consistently identified across data mining results from *N. pubescens* (NP), Open Targets (OT), and DisGeNET (DG). NetworkAnalyst further indicated that APP and AChE form direct associations with Alzheimer's disease. Although Cytoscape-based network analysis ranked only APP among the top three proteins according to betweenness centrality, STRING analysis suggested that APP can influence both AChE and BChE. Gene Ontology (GO) analysis demonstrated that APP and BChE are the most dominant proteins involved in biological processes related to Alzheimer's disease, while APP, together with CASP3 and INSR, was identified as playing a direct role in Alzheimer's disease pathogenesis. Based on these findings, APP and BChE were selected as the primary target proteins for subsequent molecular docking analysis.

GO biological process analysis (Table 6, Figure 5) confirmed the involvement of *N. pubescens* targets in key neurodegenerative mechanisms. Enriched GO terms were identified using false discovery rate (FDR) values calculated with the Benjamini–Hochberg multiple testing correction method, using the *Homo sapiens* gene set from the STRING database as the enrichment background. Terms with FDR < 0.05 were considered statistically significant. Enriched terms such as positive regulation of neuron apoptotic process (FDR = 1.33E-04, genes: PRNP, APP, CASP3, BAX, TNF) and neuron apoptotic process (FDR = 0.005081, genes: APP, CASP3, BCL2, BAX) strongly implicate the identified target network in regulating neuronal cell death, a central hallmark of Alzheimer's disease progression [32]. Furthermore, processes like learning (FDR = 0.002955, genes: BCHE, APP, INSR, PTGS2) and positive regulation of excitatory postsynaptic potential (FDR = 6.05E-04, genes: APP, GRIN2A, CHRNA7, GRIN2B) indicate potential associations with synaptic function and cognitive processes.

Complementary pathway enrichment analysis (Table 7) pinpointed specific Alzheimer's disease-related signaling cascades. The most significant pathway identified was Alzheimer's disease (hsa05010, Count = 10, FDR = 1.69E-04), which includes genes such as APP, CASP3, INSR, and TNF. These genes are reported components of pathways associated with amyloid metabolism, apoptosis, insulin signaling, and neuroinflammation in Alzheimer's disease [33]. Additional pathways such as Neuroactive ligand–receptor interaction (hsa04080) and Dopaminergic synapse (hsa04728) suggest broader neuromodulatory associations. The recurrent identification of APP and BChE across network and enrichment analyses supported their selection as representative targets for subsequent molecular docking analysis.

Table 6. Results of BP analysis of target proteins from lotus seed extract compounds.

Term	Count	FDR	Genes
GO:0043525~positive regulation of neuron apoptotic process	5	1.33E-04	**PRNP**, **APP**, **CASP3**, **BAX**, TNF
GO:2000463~positive regulation of excitatory postsynaptic potential	4	6.05E-04	**APP**, GRIN2A, CHRNA7, GRIN2B
GO:1902951~negative regulation of dendritic spine maintenance	3	0.001259	**PRNP**, **APP**, GRIN2B
GO:0050805~negative regulation of synaptic transmission	3	0.00232	**BCHE**, GABBR1, IL1B
GO:0007612~learning	4	0.002955	**BCHE**, **APP**, **INSR**, PTGS2
GO:1990535~neuron projection maintenance	3	0.003153	**PRNP**, **APP**, **INSR**
GO:0051402~neuron apoptotic process	4	0.005081	**APP**, **CASP3**, **BCL2**, **BAX**
GO:0048143~astrocyte activation	3	0.006174	**APP**, IL1B, TNF
GO:0060252~positive regulation of glial cell proliferation	3	0.008118	IL6, IL1B, TNF
GO:0051968~positive regulation of synaptic transmission, glutamatergic	3	0.01742	GRIN2A, PTGS2, GRIN2B
GO:1901216~positive regulation of neuron death	3	0.022557	**PRNP**, **APP**, GRIN2B
GO:0008542~visual learning	3	0.031854	**APP**, GRIN2A, HMGCR
GO:0050890~cognition	3	0.035118	**APP**, CHRNA7, TNF

Table 7. Results of pathways analysis of target proteins from lotus seed extract compounds.

Term	Count	FDR	Genes
hsa05010:Alzheimer disease	10	1.69E-04	**APP**, IL6, GRIN2A, IL1B, CHRNA7, **CASP3**, **INSR**, PTGS2, TNF, GRIN2B
hsa04080:Neuroactive ligand-receptor interaction	6	0.028439	GABBR2, GABBR1, GRIN2A, LEP, CHRNA7, GRIN2B
hsa04728:Dopaminergic synapse	4	0.030937	GRIN2A, MAOB, GRIN2B, SLC6A3

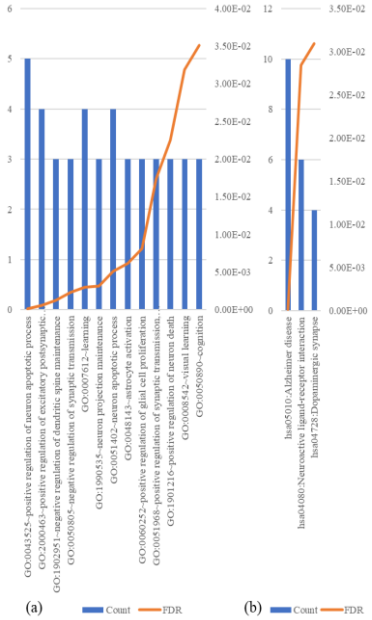

Figure 5. GO analysis **(a)** BP/Biological Process; **(b)** Pathways of *N. pubescens* seed extract target protein.

3.6. Docking analysis of APP and visualization.

Molecular docking was performed between the E2 domain of APP [7] and ten bioactive compounds from *N. pubescens*, along with a known APP inhibitory ligand, (E)-N-(pyridine-2-ylmethylene)arylamine [6]. It should be noted that PDB ID: 3UMI corresponds to the extracellular E2 domain of APP, which is structurally involved in protein-protein interactions rather than directly mediating β- or γ-secretase cleavage events [6]. In the present study, APP docking was not designed to evaluate inhibition of amyloidogenic processing directly, but rather to explore potential interactions with an Alzheimer's disease-related target protein in a broader pathological context.

The results indicated that the compounds with the highest binding affinities were Ellagic acid glucoside (EL) and 8-Demethyleucalyptin (DE) (Table 8). Both compounds exhibited more negative binding energies compared to the positive control ligand. Furthermore, only these two compounds demonstrated binding energies below the threshold of -7 kcal/mol, a value commonly used as an empirical reference for favorable binding in docking studies [34]. However, differences within this range should be interpreted cautiously, as docking scoring functions typically have an estimated error of approximately 1–2 kcal/mol.

Table 8. The binding affinity between the APP protein and 10 lotus seed compounds.

Ligand compounds	CID	Binding affinity (Kkal/mol)
(E)-N-(pyridin-2-ylmethylene)arylamine/control		-5.6
Ellagic acid glucoside	91072206	-7.9
8-Demethyleucalyptin	15715157	-7
Chalcone	637760	-6.5
9,12-Octadecadienoic acid	3931	-5.6
Galactaric acid	3037582	-4.7
2,4,6-trihydroxybenzoic acid	66520	-4.6
D-Pinitol	164619	-4.5
Propionic acid	1032	-3.5
Butanoic acid	264	-3.3

Molecular docking analysis against APP revealed that several *Nymphaea pubescens* seed compounds exhibited stronger binding affinities than the control ligand. Ellagic acid glucoside demonstrated the highest affinity (–7.9 kcal/mol), suggesting a favorable molecular interaction with the APP E2 domain. However, this interaction should not be interpreted as direct evidence of inhibition of amyloid-β production, as the E2 domain does not correspond to the β- or γ-secretase cleavage sites of APP. Polyphenolic compounds such as ellagic acid derivatives are known to bind amyloidogenic proteins through hydrogen bonding and aromatic stacking interactions, stabilizing non-toxic conformations and inhibiting Aβ oligomerization [35,36]. Nevertheless, the present docking analysis does not specifically evaluate Aβ aggregation or secretase-mediated processing, and therefore, mechanistic interpretations related to amyloidogenic inhibition remain speculative [21].

Other compounds, including 8-demethyleucalyptin (–7.0 kcal/mol) and chalcone (–6.5 kcal/mol), also displayed favorable APP binding profiles. These findings support the potential relevance of *N. pubescens* seed compounds in the broader context of Alzheimer's disease–related molecular interactions, although functional validation remains necessary [37]. Chalcones have been reported to possess various biological activities, including antioxidant and anti-inflammatory properties, which may contribute to neuroprotective effects in broader neurodegenerative contexts [38]. Furthermore, Table 9 summarizes the interactions between protein residues and both the control ligand and the compounds exhibiting the highest binding affinities. The most dominant interactions were van der Waals and hydrophobic bonds.

Residues shown in bold in the compound column correspond to control amino acid residues that are retained by the tested compounds, whereas residues in *italic* indicate changes in the type of bond formed. Additional hydrogen bond interactions were observed for some compounds compared with the control ligand, which may contribute to a favorable binding orientation within the predicted pocket. However, differences in binding affinity should be interpreted within the known limitations of docking methodologies.

Table 9. Interactions of amino acid residues in APP proteins, controls, and compounds with the best binding affinity.

Ligand	Interaction			
	Van der Waals	**Conventional Hydrogen**	**Hydrogen Carbon**	**Hydrophobic**
(E)-N-(pyridin-2-ylmethylene)arylamine/control	A: GLN454 A: THR433 A: VAL455 A: HIS458 A: MET383 A: PHE437 A: ILE451 A: HIS436 A: GLN376 A: LYS447			A: VAL440 A: VAL379
Ellagic acid glucoside	A: GLU380 **A: GLN376** A: HIS439 **A: HIS436** **A: VAL455** **A: HIS458**	*A: GLN454* A: GLU387 *A: THR433*		*A: ILE451* **A: VAL379** *A: MET383* **A: VAL440**
8-Demethyleucalyptin	**A: LYS447** **A: GLN376** **A: HIS436** **A: PHE437** **A: GLN454**		A: ARG375 *A: LYS447*	A: ARG375 *A: MET383* *A: ILE451* *A: VAL455* A: HIS439 **A: VAL379** **A: VAL440**

The α,β-unsaturated carbonyl moiety of chalcones allows interaction with residues located in structurally accessible regions of proteins. However, the current docking analysis does not directly evaluate APP–Aβ pathological cascades; therefore, these mechanistic implications remain speculative. In addition, unsaturated fatty acids such as 9,12-octadecadienoic acid showed moderate APP binding affinity (–5.6 kcal/mol), which is in line with previous reports suggesting that polyunsaturated fatty acids may influence membrane-associated APP dynamics in broader Alzheimer's disease contexts [39]. Nevertheless, the present docking analysis does not directly assess secretase-mediated cleavage mechanisms.

Figure 6 presents a 3D visualization of the APP protein complexed with the control ligands Ellagic acid glucoside (EL) and 8-Demethyleucalyptin (DE). The figure also includes 2D interaction maps illustrating the interactions between APP amino acid residues and each of the top ligands. Visualization revealed that the interaction between APP and EL formed an unfavorable bond (highlighted in red), representing a bond at an incorrect position that may compromise the stability of the protein-ligand complex. Although ellagic acid glucoside exhibited the most negative docking score, unfavorable interactions suggest that binding orientation and interaction quality should also be considered alongside binding energy values. These findings are consistent with the target prediction analysis (Figure 1), which identified DE as a compound with potential interaction relevance toward APP. However, such predictions represent computational estimations and require experimental validation to confirm biological activity.

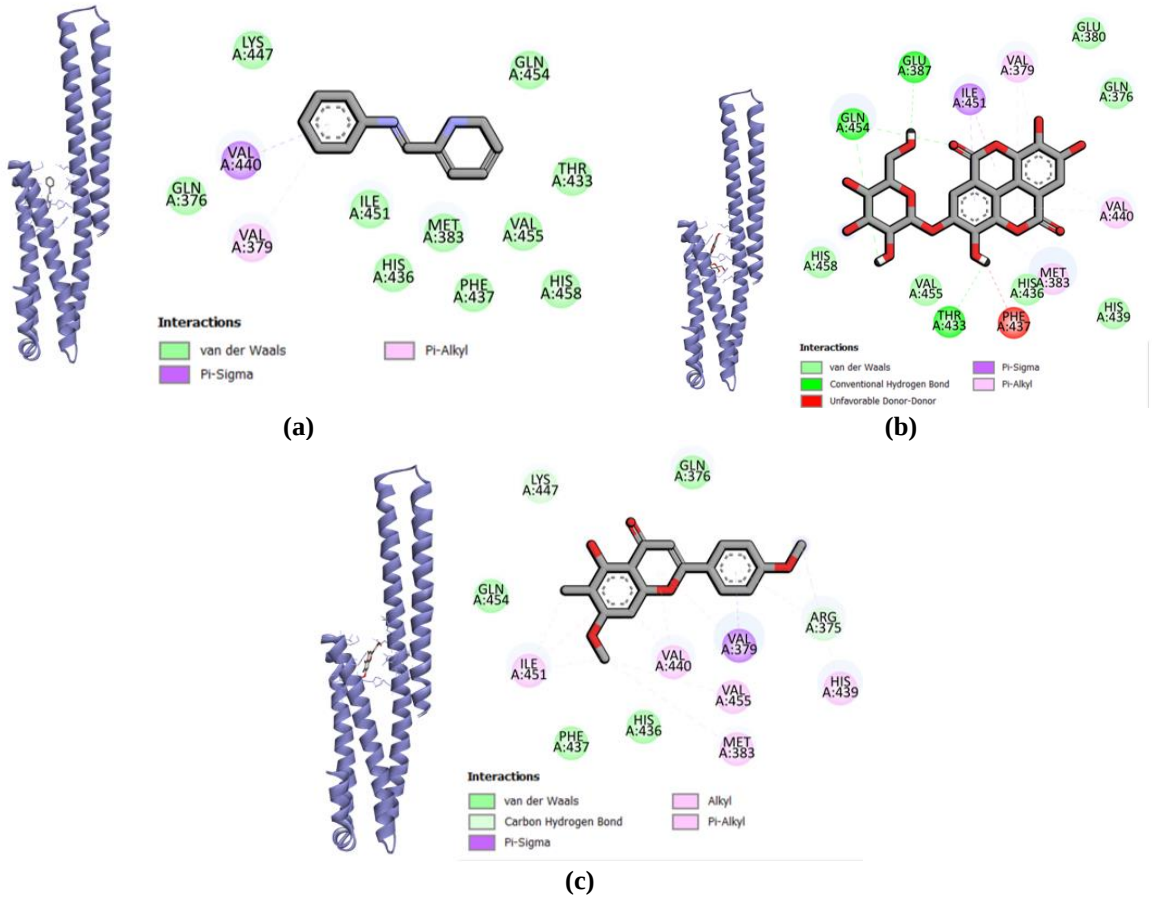

Figure 6. Visualization of docking results, **(a)** APP/(E)-N-(pyridin-2-ylmethylene)arylamine (Control); **(b)** APP/Ellagic acid glucoside; **(c)** APP/8-Demethyleucalyptin. The left part shows the 3D visualization, the right part shows the type of bond produced between the ligand and protein.

3.7. Docking analysis of BChE and visualization.

Molecular docking was performed between BChE, a cholinesterase enzyme implicated in cholinergic dysfunction in Alzheimer's disease (PDB ID: 4BDS), and ten bioactive compounds from *N. pubescens*, which were experimentally identified through LC-MS and GC-MS profiling of the seed extract. Tacrine was used as the reference inhibitor [9].

To validate the docking protocol, redocking of the co-crystallized ligand was performed, which reproduced the binding pose within the catalytic site, indicating acceptable reproduction of the experimental binding pose. Grid box dimensions were optimized to ensure full coverage of the catalytic gorge prior to docking analysis. The results indicated that the compounds with the highest binding affinities were Tacrine (control), Chalcone (CH), and 2,4,6-trihydroxybenzoic acid (TR) (Table 10). None of the tested extract compounds exhibited binding energies more negative than the positive control. Although chalcone demonstrated a binding energy below −7 kcal/mol (–7.7 kcal/mol), the difference relative to tacrine (–7.8 kcal/mol) falls within the typical scoring error margin of molecular docking algorithms (approximately 1–2 kcal/mol). Therefore, this similarity should be interpreted cautiously and does not imply equivalent inhibitory potency [34].

Table 10. Binding affinity between the BChE protein and 10 lotus seed compounds

Ligand compounds	CID	Binding Affinity (Kkal/mol)
Tacrine/Kontrol	1935	-7.8
Chalcone	637760	-7.7
2,4,6-trihydroxybenzoic acid	66520	-6

Ligand compounds	CID	Binding Affinity (Kkal/mol)
9,12-Octadecadienoic acid	3931	-5.8
D-Pinitol	164619	-5.7
Ellagic acid glucoside	91072206	-5.6
Galactaric acid	3037582	-5.4
8-Demethyleucalyptin	15715157	-4.4
Butanoic acid	264	-3.9
Propionic acid	1032	-3.3

Docking analysis against BChE suggests potential molecular interaction of selected *N. pubescens* seed constituents with the cholinergic target. Chalcone exhibited a binding affinity of –7.7 kcal/mol, numerically similar to the docking score of the reference ligand tacrine (–7.8 kcal/mol). BChE inhibition is particularly important in advanced AD, where BChE activity increases while AChE activity declines, leading to accelerated acetylcholine degradation and cognitive deterioration [40]. The predicted interaction of chalcone with BChE may indicate possible relevance within cholinergic-related pathological pathways. However, the present docking study does not evaluate enzyme inhibition kinetics, binding constants, or functional restoration of neurotransmission; therefore, docking results alone cannot confirm inhibitory activity.

Phenolic acids such as 2,4,6-trihydroxybenzoic acid (–6.0 kcal/mol) and sugar alcohols like D-pinitol (–5.7 kcal/mol) also demonstrated moderate predicted binding affinity toward BChE. These interactions should be interpreted as computational predictions rather than confirmed inhibitory activity. Importantly, BChE is not merely a cholinergic enzyme but also plays a structural role in Aβ plaque maturation. BChE has been shown to co-localize with Aβ fibrils and accelerate their conversion into more stable and neurotoxic aggregates [41,42]. However, the present study does not directly evaluate amyloid aggregation or plaque formation, and therefore, mechanistic conclusions regarding disease-modifying effects cannot be drawn.

Furthermore, Table 11 summarizes the interactions between BChE protein residues and both the control ligand and the compounds with the highest binding affinities. The most dominant interactions were van der Waals and hydrophobic bonds. Residues shown in bold in the compound column represent control amino acid residues retained by the tested compounds, while residues in *italic* indicate changes in the type of bond formed. Although several extract compounds shared interaction residues with the reference ligand, similarity in interaction patterns does not necessarily translate into comparable biological activity. Docking scores reflect predicted binding under static structural conditions and do not account for protein flexibility, solvent effects, or cellular pharmacokinetics. Additional hydrogen bond interactions were observed for some compounds compared with the control ligand, which may contribute to ligand stabilization within the predicted binding pocket.

Table 11. Interactions of amino acid residues in BChE proteins, controls, and compounds with the best binding affinity.

Ligand	Interaction			
	Van der Waals	Conventional Hydrogen	Hydrogen Carbon	Hydrophobic
Tacrine/Control	A: GLY439 A: TYR440 A: MET437 A: TRP430 A: TYR332 A: GLY116 A: TYR128	A: HIS438		A: TRP82 A: HIS438 A: ALA328

Ligand	Interaction			
	Van der Waals	**Conventional Hydrogen**	**Hydrogen Carbon**	**Hydrophobic**
	A: GLU197 A: SER198			
Chalcone	**A: GLY116** A: GLY115 **A: TYR128** **A: GLU197** **A: GLY439** *A: HIS438* A: ASP70 A: SER79 A: PHE329		*A: TRP82*	**A: TRP82** *A: TYR332* **A: ALA328**
2,4,6-trihydroxybenzoic acid	A: ILE442 **A: GLY439** A: ALA199 A: GLY115 **A: GLY116** A: GLY117 A: THR120 *A: ALA328*	*A: TYR128* *A: SER198* *A: GLU197*	*A: GLY439*	**A: TRP82** **A: HIS438**

The neuroprotective potential of *N. pubescens* seed compounds has also been associated with their reported antioxidant and anti-inflammatory activities. Propionic acid and butanoic acid, although exhibiting weaker binding affinities, have been reported to possess strong antioxidant and anti-inflammatory properties, including inhibition of reactive oxygen species (ROS) formation and lipid peroxidation [43]. Oxidative stress is a critical downstream consequence associated with Alzheimer's disease pathology, contributing to neuronal apoptosis and synaptic failure [44]. However, the present docking analysis only evaluates predicted ligand–protein interactions and does not directly assess antioxidant activity or enzyme inhibition mechanisms.

Figure 7 presents the 3D visualization of the BChE protein complexed with the control ligand, Chalcone (CH), and 2,4,6-trihydroxybenzoic acid (TR). The figure also includes 2D interaction maps illustrating the interactions between BChE amino acid residues and each of the top ligands. These docking results are consistent with the target protein prediction (Figure 1), suggesting a possible molecular interaction between CH and BChE at the predicted binding site. Meanwhile, the OC compound (9,12-Octadecadienoic acid), also predicted to interact with BChE, exhibited a binding affinity slightly lower than that of TR, indicating a moderate predicted binding affinity.

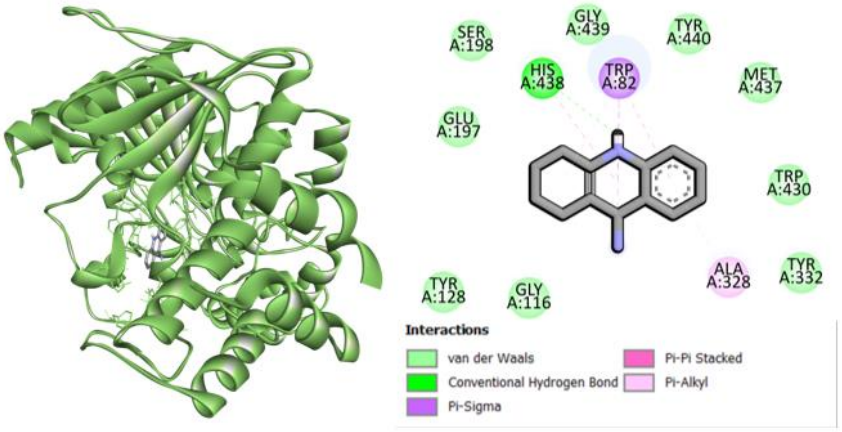

(a)

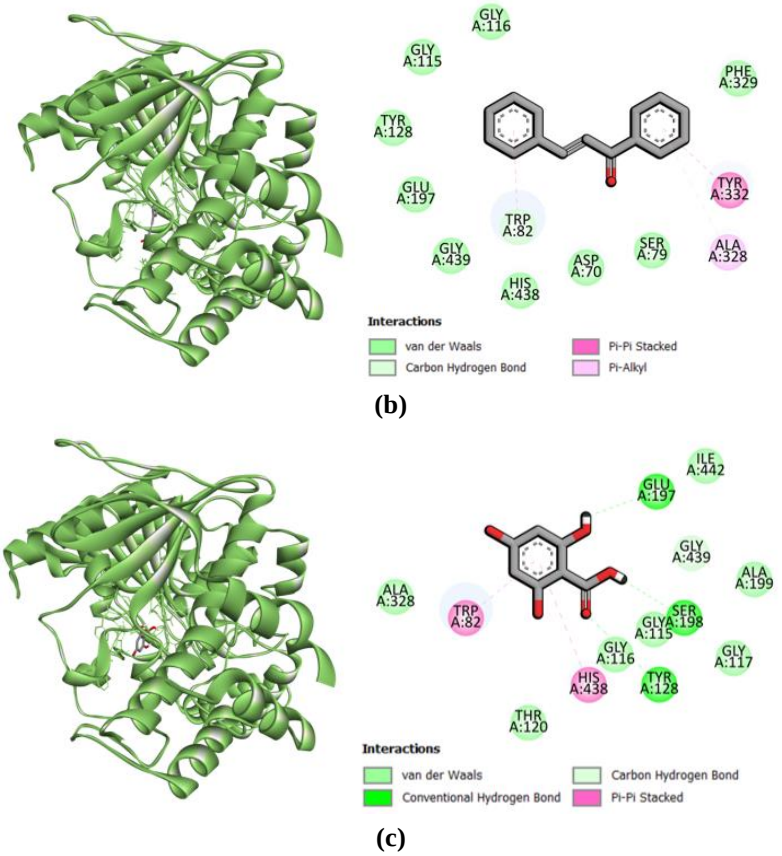

Figure 7. Visualization of docking results, **(a)** BChE/Tacrine (Control); **(b)** BChE/ Chalcone; **(c)** BChE/2,4,6-trihydroxybenzoic acid. The left part shows the 3D visualization, the right part shows the type of bond produced between the ligand and protein.

By reducing ROS generation, these short-chain fatty acids may contribute to broader neuroprotective pathways that regulate oxidative stress. Furthermore, flavonoid constituents identified in *N. pubescens* seeds, including quercetin derivatives and 8-demethyleucalyptin, are known to regulate intracellular signaling pathways, such as protein kinase and lipid kinase cascades, involved in neuronal survival, synaptic plasticity, and inflammatory responses [45]. Such mechanisms may complement potential interactions with Alzheimer's disease-related proteins, although these pathways were not directly evaluated in the present computational study.

Collectively, the integration of APP and BChE docking results with reported antioxidant and anti-inflammatory activities suggests that *N. pubescens* seed compounds may possess multitarget interaction potential within Alzheimer's disease–associated molecular pathways. Ellagic acid glucoside and chalcone emerged as compounds of interest based on predicted binding affinity and previously reported pharmacological properties. Such multitarget interaction profiles are consistent with contemporary approaches that consider the multifactorial nature of Alzheimer's disease [46]. Nevertheless, further experimental validation is necessary to confirm these in silico findings and to elucidate the precise molecular interactions in biological systems.

4. Conclusions

In silico evaluation of *Nymphaea pubescens* seed compounds provided preliminary insights into their potential interaction with Alzheimer's disease–associated targets. Molecular docking analysis revealed that ellagic acid glucoside and 8-demethyleucalyptin exhibited

strong binding affinities toward APP (−7.9 and −7.0 kcal/mol, respectively) and BChE (−5.6 and −4.4 kcal/mol), indicating potential ligand–protein interactions within the predicted binding pockets of these targets. However, docking scores represent computational predictions of binding affinity and do not directly modulate amyloid processing or cholinergic enzyme activity. Overall, the findings suggest that several compounds identified in *N. pubescens* seeds may warrant further investigation as potential molecular interactors with Alzheimer's disease–related proteins. Nevertheless, the present study is limited to computational predictions, and the biological relevance of these interactions remains to be experimentally validated. Comprehensive validation through biochemical enzyme inhibition assays, cell-based models, and in vivo studies is required before any pharmacological or therapeutic conclusions can be drawn.

Author Contributions

Conceptualization, P.S. and D.F.B.; methodology, D.F.B., P.S., and R.R.; data curation, D.F.B., P.S., and R.R.; formal analysis, D.F.B., P.S., and R.R.; writing—original draft preparation, D.F.B., P.S., and R.R.; writing—review and editing, D.F.B., P.S., and R.R. All authors contributed equally to this work and have read and agreed to the published version of the manuscript.

Institutional Review Board Statement

Not applicable.

Informed Consent Statement

Not applicable.

Data Availability Statement

Data supporting the findings of this study are available upon reasonable request from the corresponding author.

Funding

This research was supported by the Thesis Magister Research Grant from the Directorate of Research and Community Service, Ministry of Education, Culture, Research and Technology of Indonesia (Contract No. 086/E5/PG.02.00.PT/2022; Principal Investigator: Putra Santoso). The funding body had no role in the study design, data analysis, interpretation, or manuscript preparation.

Acknowledgments

The authors gratefully acknowledge the financial support from the Ministry of Education, Culture, Research, and Technology of Indonesia. The authors also thank the laboratory facilities that supported the LC-MS and GC-MS analyses conducted in this study.

Conflicts of Interest

The authors state that there is no conflict of interest.

References

1. Dementia. Available online: https://www.who.int/news-room/fact-sheets/detail/dementia (accessed on 6 February **2026**).
2. Dawkins, E.; Small, D.H. Insights into the physiological function of the β-amyloid precursor protein: beyond Alzheimer's disease. *J. Neurochem.* **2014**, *129*, 756–769, https://doi.org/10.1111/jnc.12675.
3. Swomley, A.M.; Förster, S.; Keeney, J.T.; Triplett, J.; Zhang, Z.; Sultana, R.; Butterfield, D.A. Abeta, oxidative stress in Alzheimer disease: Evidence based on proteomics studies. *Biochim. Biophys. Acta - Mol. Basis Dis.* **2014**, *1842*, 1248-1257, https://doi.org/10.1016/j.bbadis.2013.09.015.
4. Zheng, H.; Koo, E.H. The amyloid precursor protein: beyond amyloid. *Mol. Neurodegener.* **2006**, *1*, 5, https://doi.org/10.1186/1750-1326-1-5.
5. Müller, U.; Deller, T.; Korte, M. Not just amyloid: physiological functions of the amyloid precursor protein family. *Nat. Rev. Neurosci.* **2017**, *18*, 281–298, https://doi.org/10.1038/nrn.2017.29.
6. Basu Baul, T.S.; Kundu, S.; Singh, P.; Shaveta; Guedes da Silva, M.F.C. Insight into inhibition of the human amyloid beta protein precursor (APP: PDB ID 3UMI) using (E)-N-(pyridin-2-ylmethylene)arylamine (LR) models: structure elucidation of a family of ZnX2-LR complexes. *Dalton Trans.* **2015**, *44*, 2359-2369, https://doi.org/10.1039/C4DT03151B.
7. Lee, S.; Xue, Y.; Hu, J.; Wang, Y.; Liu, X.; Demeler, B.; Ha, Y. The E2 Domains of APP and APLP1 Share a Conserved Mode of Dimerization. *Biochemistry* **2011**, *50*, 5453-5464, https://doi.org/10.1021/bi101846x.
8. Darvesh, S. Butyrylcholinesterase as a Diagnostic and Therapeutic Target for Alzheimer's Disease. *Curr. Alzheimer Res.* **2016**, *13*, 1173–1177, https://doi.org/10.2174/1567205013666160404120542.
9. Nachon, F.; Carletti, E.; Ronco, C.; Trovaslet, M.; Nicolet, Y.; Jean, L.; Renard, P.-Y. Crystal structures of human cholinesterases in complex with huprine W and tacrine: elements of specificity for anti-Alzheimer's drugs targeting acetyl- and butyryl-cholinesterase. *Biochem. J.* **2013**, *453*, 393-399, https://doi.org/10.1042/BJ20130013.
10. Sathasivampillai, S.V.; Rajamanoharan, P. PHARMACOLOGICAL ACTIVITIES OF *Nymphaea pubescens* WILLD. EXTRACTS. *Acta Sci. Malays.* **2021**, *5*, 73–74, https://doi.org/10.26480/asm.02.2021.73.74.
11. Yuspihana, F.; Made, A.; Soewarno, T.S.; Komang, G.W.; Tutik, W. POTENSI BIJI DAN EKSTRAK BIJI TERATAI (*Nymphaea pubescens* Willd) Sebagai Pencegah Diare Pada Tikus Percobaan Yang Diintervensi *E.coli* Enteropatogenik. *Agritech.* **2012**, *32*, 97320.
12. Pokhrel, T.; Shrestha, D.; Dhakal, K.; Yadav, P.M.; Adhikari, A. Comparative analysis of the antioxidant and antidiabetic potential of *Nelumbo nucifera* Gaertn. and *Nymphaea lotus* L. var. *pubescens* (Willd.). *J. Chem.* **2022**, *2022*, 4258124, https://doi.org/10.1155/2022/4258124.
13. Debnath, S.; Ghosh, S.; Hazra, B. Inhibitory effect of *Nymphaea pubescens* Willd. flower extract on carrageenan-induced inflammation and CCl_4-induced hepatotoxicity in rats. *Food Chem. Toxicol.* **2013**, *59*, 485–491, https://doi.org/10.1016/j.fct.2013.06.036.
14. Aduema, W.; Munachi, I.; Akunneh-Wariso, C. Effect of Ethanol Extract Leaves of *Nymphaea Lotus* (Water Lily) on Fear and Anxiety Behaviour in Mice. *Ann. Clin. Lab. Res.* **2018**, *6*, 223.
15. Oyeyemi, I.T.; Adewole, K.E.; Gyebi, G.A. *In silico* prediction of the possible antidiabetic and anti-inflammatory targets of *Nymphaea lotus*-derived phytochemicals and mechanistic insights by molecular dynamics simulations. *J. Biomol. Struct. Dyn.* **2023**, *41*, 12225–12241, https://doi.org/10.1080/07391102.2023.2166591.
16. Ishrat, N.; Gupta, A.; Khan, M.F.; Shahab, U.; Khan, M.S.; Ahmad, N.; Kaur, K.; Ahmad, S.; Mahdi, A.A. Phytoconstituents of Nymphaea rubra flowers and their anti-diabetic metabolic targets. *Fitoterapia* **2024**, *176*, 106014, https://doi.org/10.1016/j.fitote.2024.106014.
17. Keiser, M.J.; Roth, B.L.; Armbruster, B.N.; Ernsberger, P.; Irwin, J.J.; Shoichet, B.K. Relating protein pharmacology by ligand chemistry. *Nat. Biotechnol.* **2007**, *25*, 197-206, https://doi.org/10.1038/nbt1284.
18. Piñero, J.; Ramírez-Anguita, J.M.; Saüch-Pitarch, J.; Ronzano, F.; Centeno, E.; Sanz, F.; Furlong, L.I. The DisGeNET knowledge platform for disease genomics: 2019 update. *Nucleic Acids Res.* **2020**, *48*, D845-D855, https://doi.org/10.1093/nar/gkz1021.
19. Zhou, G.; Soufan, O.; Ewald, J.; Hancock, R.E.W.; Basu, N.; Xia, J. NetworkAnalyst 3.0: a visual analytics platform for comprehensive gene expression profiling and meta-analysis. *Nucleic Acids Res.* **2019**, *47*, W234-W241, https://doi.org/10.1093/nar/gkz240.

20. Davis, A.P.; Grondin, C.J.; Johnson, R.J.; Sciaky, D.; Wiegers, J.; Wiegers, T.C.; Mattingly, C.J. Comparative Toxicogenomics Database (CTD): update 2021. *Nucleic Acids Res.* **2021**, *49*, D1138-D1143, https://doi.org/10.1093/nar/gkaa891.
21. Sherman, B.T.; Hao, M.; Qiu, J.; Jiao, X.; Baseler, M.W.; Lane, H.C.; Imamichi, T.; Chang, W. DAVID: a web server for functional enrichment analysis and functional annotation of gene lists (2021 update). *Nucleic Acids Res.* **2022**, *50*, W216-W221, https://doi.org/10.1093/nar/gkac194.
22. Xiong, G.; Wu, Z.; Yi, J.; Fu, L.; Yang, Z.; Hsieh, C.; Yin, M.; Zeng, X.; Wu, C.; Lu, A.; Chen, X.; Hou, T.; Cao, D. ADMETlab 2.0: an integrated online platform for accurate and comprehensive predictions of ADMET properties. *Nucleic Acids Res.* **2021**, *49*, W5-W14, https://doi.org/10.1093/nar/gkab255.
23. Zhao, L.; Ciallella, H.L.; Aleksunes, L.M.; Zhu, H. Advancing computer-aided drug discovery (CADD) by big data and data-driven machine learning modeling. *Drug Discov. Today* **2020**, *25*, 1624–1638, https://doi.org/10.1016/j.drudis.2020.07.005.
24. Yuan, S.; Ma, T.; Zhang, Y.-N.; Wang, N.; Baloch, Z.; Ma, K. Novel drug delivery strategies for antidepressant active ingredients from natural medicinal plants: the state of the art. *J. Nanobiotechnol.* **2023**, *21*, 391, https://doi.org/10.1186/s12951-023-02159-9.
25. Singh, A.; Kukreti, R.; Saso, L.; Kukreti, S. Oxidative Stress: A Key Modulator in Neurodegenerative Diseases. *Molecules* **2019**, *24*, 1583, https://doi.org/10.3390/molecules24081583.
26. Rusek, M.; Smith, J.; El-Khatib, K.; Aikins, K.; Czuczwar, S.J.; Pluta, R. The Role of the JAK/STAT Signaling Pathway in the Pathogenesis of Alzheimer's Disease: New Potential Treatment Target. *Int. J. Mol. Sci.* **2023**, *24*, 864, https://doi.org/10.3390/ijms24010864.
27. Perucca, E.; Bialer, M.; White, H.S. New GABA-Targeting Therapies for the Treatment of Seizures and Epilepsy: I. Role of GABA as a Modulator of Seizure Activity and Recently Approved Medications Acting on the GABA System. *CNS Drugs* **2023**, *37*, 755–779, https://doi.org/10.1007/s40263-023-01027-2.
28. Pinzi, L.; Lherbet, C.; Baltas, M.; Pellati, F.; Rastelli, G. In Silico Repositioning of Cannabigerol as a Novel Inhibitor of the Enoyl Acyl Carrier Protein (ACP) Reductase (InhA). *Molecules* **2019**, *24*, 2567, https://doi.org/10.3390/molecules24142567.
29. Wu, L.; Hao, Y.; Dai, C.; Zhang, Z.; Ijaz, M.; Ibrahim, S.M.; Murtaza, G.; Yao, Z. Network Pharmacological Study of *Achyranthis bidentatae* Radix Effect on Bone Trauma. *Biomed Res. Int.* **2021**, *2021*, 5692039, https://doi.org/10.1155/2021/5692039.
30. Zhou, Z.; Zhang, Y.; Liu, S.; Tang, H.; Yang, L.; Lu, Y.; Liao, J.; Zhang, S.; Chen, Z.; Yang, L. Ferroptosis in Alzheimer's disease: molecular mechanisms and advances in therapeutic strategies. *Front. Neurosci.* **2026**, *19*, 1673315, https://doi.org/10.3389/fnins.2025.1673315.
31. Zhou, Y.; Zhang, Y.; Lian, X.; Li, F.; Wang, C.; Zhu, F.; Qiu, Y.; Chen, Y. Therapeutic target database update 2022: facilitating drug discovery with enriched comparative data of targeted agents. *Nucleic Acids Res.* **2022**, *50*, D1398-D1407, https://doi.org/10.1093/nar/gkab953.
32. Dhapola, R.; Hota, S.S.; Sarma, P.; Bhattacharyya, A.; Medhi, B.; Reddy, D.H. Recent advances in molecular pathways and therapeutic implications targeting neuroinflammation for Alzheimer's disease. *Inflammopharmacology* **2021**, *29*, 1669-1681, https://doi.org/10.1007/s10787-021-00889-6.
33. You, G.; Yao, J.; Liu, Q.; Li, N. The Strategies for Treating "Alzheimer's Disease": Insulin Signaling May Be a Feasible Target. *Curr. Issues Mol. Biol.* **2022**, *44*, 6172-6188, https://doi.org/10.3390/cimb44120421.
34. Trott, O.; Olson, A.J. AutoDock Vina: Improving the speed and accuracy of docking with a new scoring function, efficient optimization, and multithreading. *J. Comput. Chem.* **2010**, *31*, 455–461, https://doi.org/10.1002/jcc.21334.
35. Pandey, K.B.; Rizvi, S.I. Plant Polyphenols as Dietary Antioxidants in Human Health and Disease. *Oxid. Med. Cell. Longev.* **2009**, *2*, 270–278, https://doi.org/10.4161/oxim.2.5.9498.
36. Ahmadi, S.; Javid, H. Novel formulations of ellagic acid for the improvement of antimicrobial, antioxidant, anticancer, antidiabetic, and neuroprotective applications. *Nano Micro Biosyst.* **2023**, *2*, 31–35, https://doi.org/10.22034/nmbj.2023.388479.1015.
37. Zhang, X.; Rakesh, K.P.; Bukhari, S.N.A.; Balakrishna, M.; Manukumar, H.M.; Qin, H.-L. Multi-targetable chalcone analogs to treat deadly Alzheimer's disease: Current view and upcoming advice. *Bioorg. Chem.* **2018**, *80*, 86-93, https://doi.org/10.1016/j.bioorg.2018.06.009.
38. Królicka, E.; Kieć-Kononowicz, K.; Łażewska, D. Chalcones as Potential Ligands for the Treatment of Parkinson's Disease. *Pharmaceuticals* **2022**, *15*, 847, https://doi.org/10.3390/ph15070847.
39. Bazinet, R.P.; Layé, S. Polyunsaturated fatty acids and their metabolites in brain function and disease. *Nat. Rev. Neurosci.* **2014**, *15*, 771–785, https://doi.org/10.1038/nrn3820.

40. Vecchio, I.; Sorrentino, L.; Paoletti, A.; Marra, R.; Arbitrio, M. The state of the art on acetylcholinesterase inhibitors in the treatment of Alzheimer's disease. *J. Cent. Nerv. Syst. Dis.* **2021**, *13*, 11795735211029113, https://doi.org/10.1177/11795735211029113.
41. Zueva, I.V.; Vasilieva, E.A.; Gaynanova, G.A.; Moiseenko, A.V.; Burtseva, A.D.; Boyko, K.M.; Zakharova, L.Y.; Petrov, K.A. Can Activation of Acetylcholinesterase by β-Amyloid Peptide Decrease the Effectiveness of Cholinesterase Inhibitors? *Int. J. Mol. Sci.* **2023**, *24*, 16395, https://doi.org/10.3390/ijms242216395.
42. Majdi, A.; Sadigh-Eteghad, S.; Rahigh Aghsan, S.; Farajdokht, F.; Vatandoust, S.M.; Namvaran, A.; Mahmoudi, J. Amyloid-β, tau, and the cholinergic system in Alzheimer's disease: seeking direction in a tangle of clues. *Rev. Neurosci.* **2020**, *31*, 391–413, https://doi.org/10.1515/revneuro-2019-0089.
43. Al-Huqail, A.A.; Elgaaly, G.A.; Ibrahim, M.M. Identification of bioactive phytochemical from two *Punica* species using GC–MS and estimation of antioxidant activity of seed extracts. *Saudi J. Biol. Sci.* **2018**, *25*, 1420–1428, https://doi.org/10.1016/j.sjbs.2015.11.009.
44. Butterfield, D.A.; Boyd-Kimball, D. Oxidative Stress, Amyloid-β Peptide, and Altered Key Molecular Pathways in the Pathogenesis and Progression of Alzheimer's Disease. *J. Alzheimers Dis.* **2018**, *62*, 1345–1367, https://doi.org/10.3233/JAD-170543.
45. Angelova, P.R.; Esteras, N.; Abramov, A.Y. Mitochondria and lipid peroxidation in the mechanism of neurodegeneration: Finding ways for prevention. *Med. Res. Rev.* **2021**, *41*, 770–784, https://doi.org/10.1002/med.21712.
46. Cummings, J.; Lee, G.; Ritter, A.; Sabbagh, M.; Zhong, K. Alzheimer's disease drug development pipeline: 2019. *Alzheimers Dement.: Transl. Res. Clin. Interv.* **2019**, *5*, 272–293, https://doi.org/10.1016/j.trci.2019.05.008.

Publisher's Note & Disclaimer